

## TRI-BAND METAMATERIAL-INSPIRED MONOPOLE ANTENNA WITH MODIFIED S-SHAPED RESONATOR

G. Du, X. Tang, and F. Xiao <sup>†</sup>

The EHF Key Laboratory of Fundamental Science  
School of Electronic Engineering  
University of Electronic Science and Technology of China  
Chengdu, Sichuan 611731, China

**Abstract**—In this paper, a tri-band metamaterial-inspired monopole antenna is proposed for multi-band wireless applications. A metamaterial consisting of three dual-band modified S-shaped resonators (MSRs) is directly connected to a regular monopole element, which can not only support the two WiFi bands but also bring the resonant frequency of monopole element down to the WiMAX band while the length of the antenna is maintained unchanged. The simulated and measured results verify our design for the wireless applications.

### 1. INTRODUCTION

To satisfy the demand of two commonly used wireless communication systems, the WiFi and the WiMAX, a compact multi-band antenna is desirable. Planar monopole antennas are regarded as good alternatives for wireless applications because some advantages such as bandwidth, omnidirectional radiation pattern, low profile and low cost. Furthermore, it can also offer a chance of multi-band operations [1–3]. In order to achieve multi-band operation, several traditional approaches are used. In [4, 5], multi-branched strips are added to the monopole design to stimulate multiple resonant bands, which generally leads to a large volume or requires a large ground plane. In [6, 7], slots are cut into radiator or ground plane to excite multiple resonant modes. Recently, metamaterials have been exhibiting their

---

*Received 15 March 2011, Accepted 11 April 2011, Scheduled 13 April 2011*

Corresponding author: Fei Xiao (fxiao316@gmail.com).

<sup>†</sup> G. Du is also with School of Electronic Engineering, Chengdu University of Information Technology, Chengdu, Sichuan 610225, China.

potentiality in the implementation of resonant antenna [8–10], which also provide a conceptual route for multi-band operations [11–16]. Generally speaking, transmission-line metamaterials antenna suffers from narrow band or structural complexity due to via or other extra line connected to ground in order to get shunt inductance that is necessary for transmission-line metamaterials. In [16], a compact tri-band monopole antenna is proposed using reactive loading and a “defected” ground-plane, which requires a longer feed line and then leads to a large size.

In this paper, a tri-band monopole antenna is proposed, which employs a metamaterial structure consisting of three dual-band MSRs regarded as reactive loading. The resonators not only allow the monopole antenna to directly cover both the WiFi bands 2.40–2.48 GHz and 5.15–5.8 GHz based on its self-resonances but also pull the monopole’s self-resonant frequency down to the WiMAX band 3.30–3.80 GHz. In addition, because of a single layer and no grounded via, the antenna is easier to be fabricated. The simulated and measured results are presented for verification.

## 2. ANTENNA DESIGN

The configuration of the proposed antenna is shown in Figure 1, which is designed on a CER\_10 ( $\epsilon_r = 9.5$ ,  $\tan \delta = 0.001$ ) substrate with a thickness of 0.635 mm. The antenna is comprised of a monopole element and a metamaterial structure. In the metamaterial

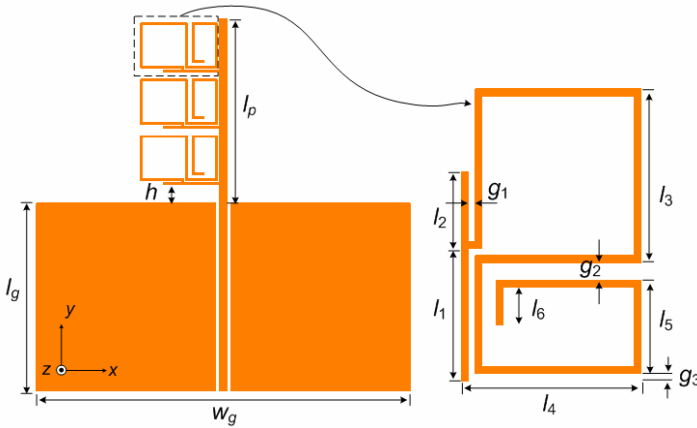


**Figure 1.** The configuration of the proposed tri-band metamaterial-inspired monopole antenna.

structure, three MSR are arranged in a  $1 \times 3$  array and directly connected to the monopole element. The MSR consists of a straight metal line and the modified S-shaped metal line, which are both printed on the same side, instead of two sides of the substrate, to construct the simple metamaterial unit cell. In order to determine its resonant characteristics through electromagnetic simulation, the MSR is individually placed within an air box. To approximate infinite periodically arranged unit cells, the perfect electric conductor (PEC) and perfect magnetic conductor (PMC) boundary conditions are set for the top/lower faces and front/back faces of the box, perpendicular to  $x$ -axis and  $z$ -axis respectively. The faces perpendicular to the  $y$ -axis are modeled as the input/output ports. Then, the MSR is excited by an electromagnetic wave with propagation vector ( $\mathbf{k}$ ) along  $y$ -axis, electric field vector ( $\mathbf{E}$ ) along the  $x$ -axis and magnetic field vector ( $\mathbf{H}$ ) along  $z$ -axis, as shown in Figure 2.

The magnitude of the transmission parameter  $S_{21}$  for the MSR is calculated by the commercial electromagnetic solver HFSS. For example, the detailed dimensions of the MSR are listed in Table 1. The width of all the lines is chosen as 0.1 mm. Finally, the whole size

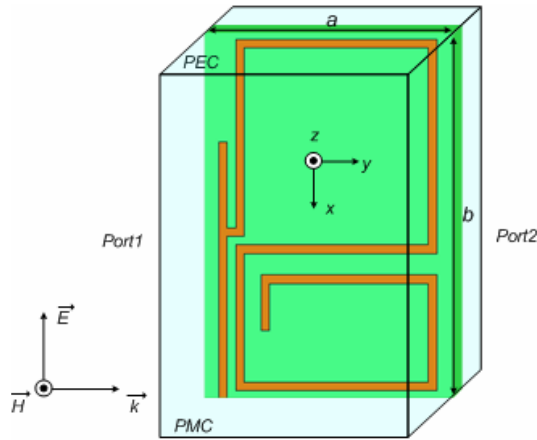


**Figure 2.** The configuration of the MSR.

**Table 1.** MSR design dimensions (unit: mm).

$l_1$	1.9	$l_4$	2.6	$g_1$	0.1
$l_2$	1.1	$l_5$	1.35	$g_2$	0.2
$l_3$	2.5	$l_6$	0.55	$g_3$	0.1

of the resonator is  $a \times b = 3.0 \times 4.3 \text{ mm}^2$  (or  $1/40.8\lambda_0 \times 1/27.8\lambda_0$  at 2.46 GHz). The simulated results are shown in Figure 3, i.e., the black solid line, where two resonant frequencies 2.0 and 4.57 GHz can be clearly distinguished. In addition, the resonant frequencies of the MSR can be flexibly shifted by changing some parameters. For example, if  $l_1 = 1.5 \text{ mm}$ ,  $l_3 = 2.0 \text{ mm}$  and  $l_5 = 0.95 \text{ mm}$ , the two resonant frequencies increase to 2.27 and 5.24 GHz as represented by the red dashed line in Figure 3. In fact, around the two resonant frequencies, the MSR exhibits the feature of negative refractive index. Figure 4 shows the effective index retrieved from the simulated  $S$ -parameters using the parametric retrieval algorithm [17] for the MSR when the dimensions in Table 1 are used. We can observe that the effective index has the negative real part around 2.0 and 4.57 GHz.

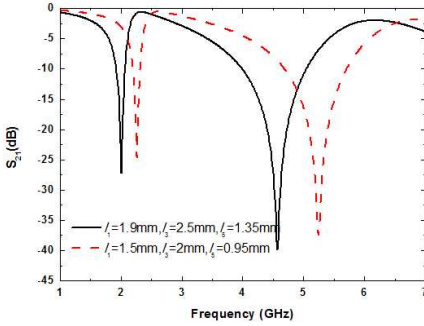


**Figure 3.** The simulated magnitude of  $S_{21}$  for the MSR.

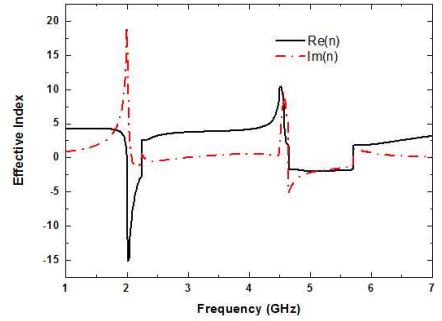


**Figure 4.** The effective index retrieved from the simulated  $S$ -parameters for the MSR with dimensions in Table 1.

Three MSRs comprise a metamaterial structure and then are directly connected to the monopole element. As a dual-band reactive loading, this metamaterial structure not only forces the monopole antenna to resonate at both the lower WiFi band and the upper WiFi band due to its own dual-band characteristics but also move the self-resonant frequency of the monopole element down to MiMAX band.

According to the general design guideline that the lowest resonance is determined when the length of the monopole is approximately  $\lambda_g/4$ , in our antenna design, the length of the monopole element is chosen as  $l_p = 9.8 \text{ mm}$  (or  $1/12.5\lambda_0$  at 2.46 GHz), which results in the lowest resonance occurring at 4.27 GHz. The overall size of the antenna is  $20 \times 24 \text{ mm}^2$  including the ground plane  $l_g \times w_g =$

$10 \times 24 \text{ mm}^2$ . The distance between the metamaterial unit cell and the ground plane is  $h = 1 \text{ mm}$ . The antenna is fed by a  $50 \Omega$  coplanar waveguide (CPW) transmission-line with the slot width  $0.2 \text{ mm}$  and the center conductor width  $0.45 \text{ mm}$ , which can be easily integrated with the other CPW-based microwave circuits.

### 3. RESULTS AND DISCUSSION

Figure 5 shows photograph of the fabricated tri-band monopole antenna. The antenna is measured by a network analyzer Rohde Schwarz ZVB20. The HFSS-simulated and measured magnitudes of  $S_{11}$  are shown in Figure 6, where three operating frequency bands are quite obvious for the proposed antenna. The antenna exhibits the characteristics of the tri-band operation, i.e., a measured  $-10 \text{ dB}$  bandwidth of  $100 \text{ MHz}$  for the lower WiFi band from  $2.40 \text{ GHz}$

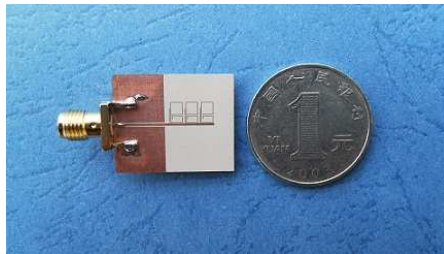


**Figure 5.** Fabricated prototype of proposed Tri-band MTM-inspired small.

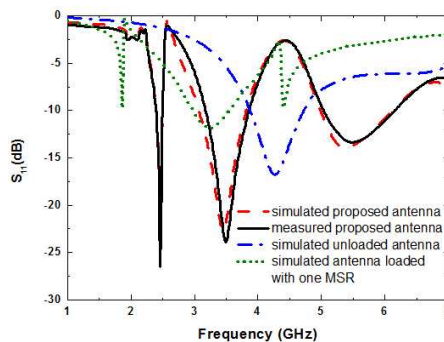


**Figure 6.** Simulated and measured  $S_{11}$  for the proposed tri-band antenna compared with unloaded monopole antenna and monopole antenna loaded with one MSR.

to 2.50 GHz, a bandwidth of 1.11 GHz from 5.04 GHz to 6.15 GHz covering the upper WiFi and the WiMAX band with 680 MHz bandwidth from 3.18 GHz to 3.86 GHz. Compared with the unloaded monopole antenna, the metamaterial-inspired monopole antenna not only provides two WiFi bands but also moves the resonant frequency of the monopole element from 4.27 GHz down to 3.45 GHz which just falls in the WiMAX band. If there is only one MSR connected to the monopole element, the resonant strength will become weaker and resonant frequencies will be reduced down, although tri-band characteristics also exist, as shown in Figure 6.

Figure 7 shows the HFSS simulation results for the different current distributions on a single MSR at 2.46 GHz, 3.45 GHz and 5.39 GHz, respectively. In practice, the MSR has to be connected to the monopole element, whose boundaries should be changed into radiation boundary instead of PEC and PMC as shown as in Figure 2. Therefore, the MSR will introduce the resonant frequencies 2.46 GHz and 5.39 GHz to the antenna after they are connected to the monopole element, which is different from the resonant frequencies 2.0 GHz and 4.57 GHz of a single MSR in Figure 3. Figure 7 indicates that the resonant frequency 2.46 GHz depends on the overall size of the resonator while the other frequency 5.39 GHz depends on the dimensions of the lower part of the resonator.

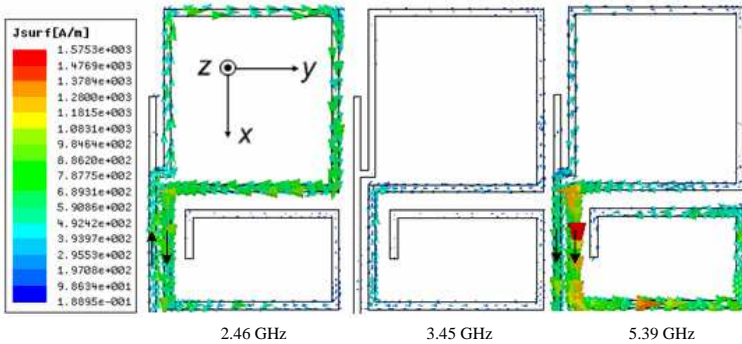


**Figure 7.** Simulated surface current distribution on MSR of tri-band monopole antenna at three resonant frequencies.

The measured and simulated radiation patterns for the proposed tri-band metamaterial-inspired monopole antenna are plotted in Figures 8, 9 and 10, where the three principle planes at the frequencies of 2.46 GHz, 3.45 GHz and 5.39 GHz are shown respectively. Using the gain comparison method, the measured maximum gain of the proposed

antenna is 0.76, 0.86 and 1.58 at the frequencies of 2.46, 3.45 and 5.39 GHz respectively. When it is just a monopole element, the gain is 1.26. Figure 8 shows the radiation pattern at 2.46 GHz for the  $E$ -plane (the  $yz$ -plane and the  $xy$ -plane) and the  $H$ -plane (the  $xz$ -plane). A  $y$ -directed liner  $E$ -field polarization is exhibited due to the  $y$ -directed current distributed on the MSR at 2.46 GHz as shown in Figure 7. The neighboring  $x$ -directed currents on the straight metal line and the lower part of modified S-shaped metal line are in opposite direction, which only leads to a weak cross-polarization in the  $yz$ -plane. Contrarily, at 5.39 GHz, the neighboring  $x$ -directed currents are in the same direction, which makes contribution to a stronger cross-polarization in the  $yz$ -plane. Meanwhile, the intense  $y$ -directed current

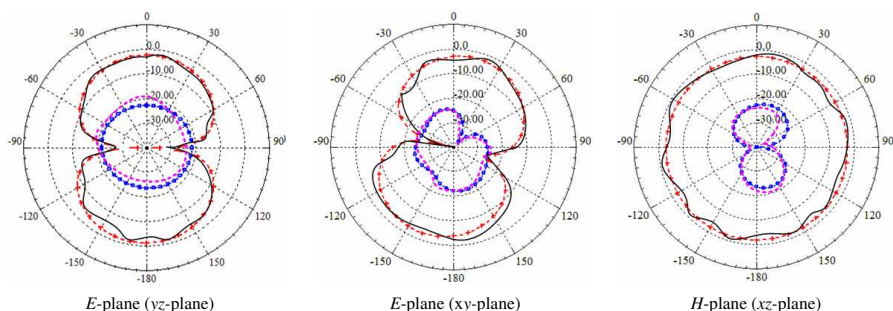


**Figure 8.** Simulated and measured radiation patterns for proposed tri-band antenna at 2.46 GHz. - + - simulated copolarization, — measured copolarization, -- simulated cross-polarization, and - - - measured cross-polarization.

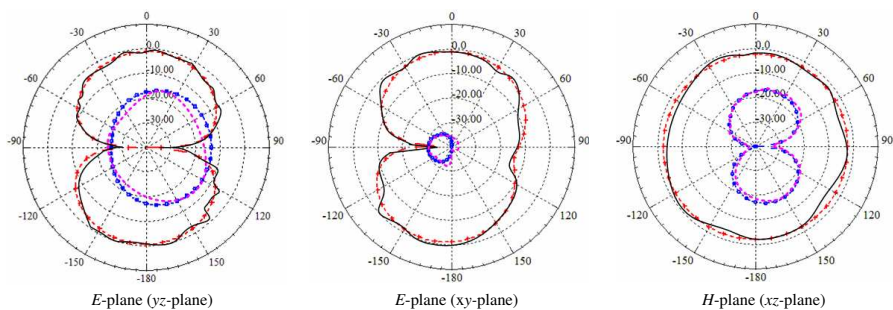


**Figure 9.** Simulated and measured radiation patterns for proposed tri-band antenna at 3.45 GHz. - + - simulated copolarization, — measured copolarization, -- simulated cross-polarization, and - - - measured cross-polarization.

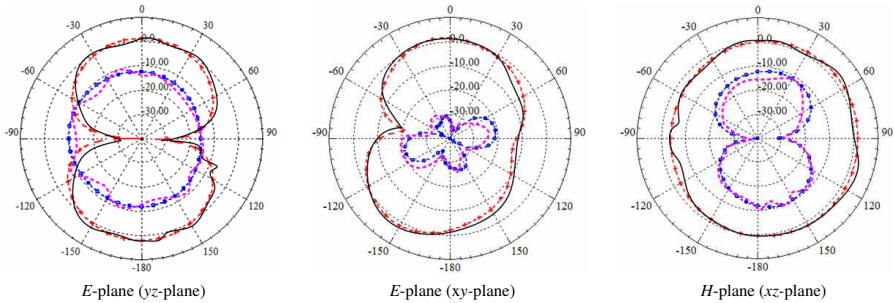


**Figure 10.** Simulated and measured radiation patterns for proposed tri-band antenna at 5.39 GHz. - + - simulated copolarization, — measured copolarization, -- simulated cross-polarization, and - - - measured cross-polarization.

distribution at 5.39 GHz in Figure 7 corresponds to the copolarization of the radiation pattern in the  $yz$ -plane shown in Figure 10, which has a maximum gain 1.58, 3.2 dBi greater than that at 2.46 GHz in Figure 8. However, different from the two WiFi bands, the current on the MSR at 3.45 GHz is very small which makes minimum contribution to the radiation. The radiation at 3.45 GHz is mainly created by the current on the monopole element along the  $y$ -direction. The current distributions in Figure 7 and the radiation patterns indicate that the proposed antenna can radiate in the WiFi upper band and the lower band owing to the dual-band resonance of the MSR which also inspires the antenna to operate in the WiMAX band though the coupling effect between them.

#### 4. CONCLUSION

A tri-band MTM-inspired antenna is proposed for the WiFi and WiMAX applications. The antenna consists of a CPW-fed monopole element and the MSRs. The MSRs introduce another two resonances in the lower and upper WiFi bands respectively, meanwhile they also shift the resonant frequency of the monopole element down to the WiMAX band through adjusting the coupling strength between them. The antenna exhibits the monopole-like radiation patterns at three bands. The simulated and measured results show the proposed antenna might be useful for multi-band communication systems.

## ACKNOWLEDGMENT

This work was supported by the National Science Foundation for Young Scientists of China (Grant No. 60801028).

## REFERENCES

1. Chen, H.-M., Y.-F. Lin, C.-C. Kuo, and K.-C. Huang, "A compact dual-band microstrip-fed monopole antenna," *Proc. IEEE Antennas and Propagation Society Int. Symp. Digest*, Vol. 2, 124–127, 2001.
2. Chen, S.-B., Y.-C. Jiao, W. Wang, and F.-S. Zhang, "Modified T-shaped planar monopole antennas for multiband operation," *IEEE Trans. Microw. Theory Tech.*, Vol. 54, 3267–3270, 2006.
3. Liao, W.-J., S.-H. Chang, and L.-K. Li, "A compact planar multiband antenna for integrated mobile devices," *Progress In Electromagnetics Research*, Vol. 109, 1–16, 2010.
4. Jaw, J. L. and J. K. Chen, "CPW-fed hook-shaped strip antenna for dual wideband operation," *Journal of Electromagnetic Waves and Applications*, Vol. 22, No. 13, 1809–1818, 2008.
5. Ge, Y., K. Esselle, and T. Bird, "Compact triple-arm multi-band monopole antenna," *Proc. IEEE Int. Workshop: Antenna Technology Small Antennas and Novel Metamaterials*, 172–175, 2006.
6. Wong, K.-L., G.-Y. Lee, and T.-W. Chiou, "A low-profile planar monopole antenna for multiband operation of mobile handsets," *IEEE Trans. Antennas Propag.*, Vol. 51, No. 1, 121–125, 2003.
7. Lin, C.-I. and K.-L. Wong, "Printed monopole slot antenna for internal multiband mobile phone antenna," *IEEE Trans. Antennas Propag.*, Vol. 55, No. 12, 3690–3697, 2007.
8. Eleftheriades, G. V., A. Grbic, and M. Antoniadis, "Negative-refractive-index transmission-line metamaterials and enabling electromagnetic applications," *IEEE Antennas and Propagation Society Int. Symp. Digest*, 1399–1402, 2004.
9. Wu, B.-I., W. Wang, J. Pacheco, X. Chen, T. M. Grzegorzczak, and J. A. Kong, "A study of using metamaterials as antenna substrate to enhance gain," *Progress In Electromagnetics Research*, Vol. 51, 295–328, 2005.
10. Hwang, R.-B., H.-W. Liu, and C.-Y. Chin, "A metamaterial-based E-plane horn antenna," *Progress In Electromagnetics Research*, Vol. 93, 275–289, 2009.
11. Yu, A., F. Yang, and A. Elsherbeni, "A dual band circularly

- polarized ring antenna based on composite right and left handed metamaterials,” *Progress In Electromagnetics Research*, Vol. 78, 73–81, 2008.
12. Si, L.-M. and X. Lv, “CPW-FED multi-band omni-directional planar microstrip antenna using composite metamaterial resonators for wireless communications,” *Progress In Electromagnetics Research*, Vol. 83, 133–146, 2008.
  13. Li, L.-W., Y.-N. Li, T.-S. Yeo, et al., “A broadband and high-gain metamaterial microstrip antenna,” *Appl. Phys. Lett.*, Vol. 96, No. 16, 1641017, 2010.
  14. Antoniadis, M. A. and G. V. Eleftheriades, “A broadband dual-mode monopole antenna using NRI-TL metamaterial loading,” *IEEE Antennas Wireless Propag. Lett.*, No. 8, 258–261, 2009.
  15. Niu, J.-X., “Dual-band dual-mode patch antenna based on resonant-type metamaterial transmission line,” *Electron. Lett.*, Vol. 46, No. 4, 266–268, 2010.
  16. Zhu, J., M. A. Antoniadis, and G. V. Eleftheriades, “A compact tri-band monopole antenna with single-cell metamaterial loading,” *IEEE Trans. Antennas Propag.*, Vol. 54, No. 8, 1031–1038, 2010.
  17. Smith, D. R., D. C. Vier, T. Koschny, and C. M. Soukoulis, “Electromagnetic parameter retrieval from inhomogeneous metamaterials,” *Phys. Rev. E*, Vol. 71, 036617, 2005.